Cretaceous Research 56 (2015) 110–118

Contents lists available at ScienceDirect

Cretaceous Research

journal homepage: www.elsevier.com/locate/CretRes

Mid-Cretaceous radiolarian faunas from the Ashin Ophiolite (western Central-East Iranian Microcontinent)

Nargess Shirdashtzadeh [a, *], Sarah Kachovich [b], Jonathan C. Aitchison [b], Ramin Samadi [c]

[a] Department of Geology, Faculty of Science, University of Isfahan, Isfahan, Iran
[b] School of Geography, Planning and Environmental Management, The University of Queensland, St Lucia, QLD 4072, Australia
[c] Department of Geology, Science and Research Branch, Islamic Azad University, Tehran, Iran

ARTICLE INFO

Article history:
Received 17 December 2014
Accepted in revised form 10 April 2015
Available online

Keywords:
Cretaceous
Radiolarian chert
Ashin ophiolitic mélange
Central-East Iranian Microcontinent

ABSTRACT

The Ashin ophiolitic mélange crops out in the west of the Central-East Iranian Microcontinent (CEIM). Accurate dating the deep-water radiolarian chert deposits associated with this ophiolite provide valuable data to constrain the stratigraphic and paleotectonic evolution this Neo-Tethyan oceanic basin. Chert nodules within Upper Cretaceous limestones and chert layers overlying pillow lavas of this ophiolite were collected and examined in detail for the first time. Radiolarians indicate that the cherts accumulated in the mid-Cretaceous in a deep marine setting within the eastern branch of the Tethyan Ocean in Iran. Two distinct radiolarian faunas, one mid-Albian (~107 Ma) the other Turonian (~94 Ma) were recovered. The radiolarian microfossil ages are consistent with radiometric ages previously obtained from associated plagiogranites and quartz keratophyre. This study indicates that mid-Cretaceous radiolarian assemblages from the western CEIM are similar to other radiolarian faunas reported from Cretaceous ophiolites in Greece, Turkey, Iran (Outer Zagros Ophiolitic Belt in Iran, e.g. Khoy, Kermanshah, Neyriz, and Soulabest), and southern Tibet in China.

1. Introduction

Neo-Tethyan Ocean relics are found from New Zealand westward to southern Tibet, Iran, Turkey, Greece, southern Europe and the North Atlantic oceanic basin (Chen et al., 2007; Jansa and Hu, 2009). The Cimmerian terranes of present-day Iran migrated from southern Gondwana as a consequence of the opening of the western branch of the Neo-Tethyan Ocean between the Iranian and Arabian plates (Fig. 1A), in the Early to Middle Permian to Early Triassic (e.g. Agard et al., 2011, and references therein). Glennie (1992), Torabi (2004), Reichert (2007), Shirdashtzadeh et al. (2010, 2011, 2014) considered the eastern branch of the Neo-Tethyan Ocean (or Nain-Baft Ocean in Ghasemi and Talbot, 2006, and Shirdashtzadeh et al., 2011), opened from southeast Turkey to Oman and separated the Sanandaj-Sirjan and Central Iranian plates (Fig. 1A), from the approximately Early Jurassic to the late Early Cretaceous-Paleocene. Timing of opening of this Neo-Tethyan Ocean branch is not well constrained. Closure of branches of the Neo-Tethyan Ocean in Late Cretaceous times resulted in emplacement of the Zagros (e.g. Kermanshah, Neyriz) to Oman ophiolites along the western branch of Neo-Tethys in Iran, as well as Ashin, Nain to Baft ophiolites in the west of the CEIM, along the eastern branch of Neo-Tethys in Iran (Fig. 1A–C).

The Mesozoic ophiolites of Iran provide important data on how the Neo-Tethyan oceanic basin formed and disappeared. Closure of the eastern branch of the Neo-Tethyan Ocean in the Late Cretaceous resulted in formation of ophiolitic mélange of Ashin (=Ashin-Zavar) along the Nain – Baft to Dorouneh faults (Fig. 1D). Geological evidence indicates that the oceanic basin of eastern branch of Neo-Tethys was long-lived (~150–100 Ma) (Shirdashtzadeh et al., 2014). It is believed that the Ashin Ophiolite was emplaced before the Paleocene at some time during the Late Cretaceous (Stocklin, 1974; Stoneley, 1975), because Paleocene-Eocene deposits cover it. Sharkovski et al. (1984) reported a 98 Ma (Cenomanian) age for some of the latest magmatism (K–Ar dating of plagiogranite and quartz keratophyre) in the Ashin Ophiolite.

* Corresponding author. Tel.: +98 913 3015905.
E-mail address: nshirdasht@gmail.com (N. Shirdashtzadeh).

http://dx.doi.org/10.1016/j.cretres.2015.04.003
0195-6671/

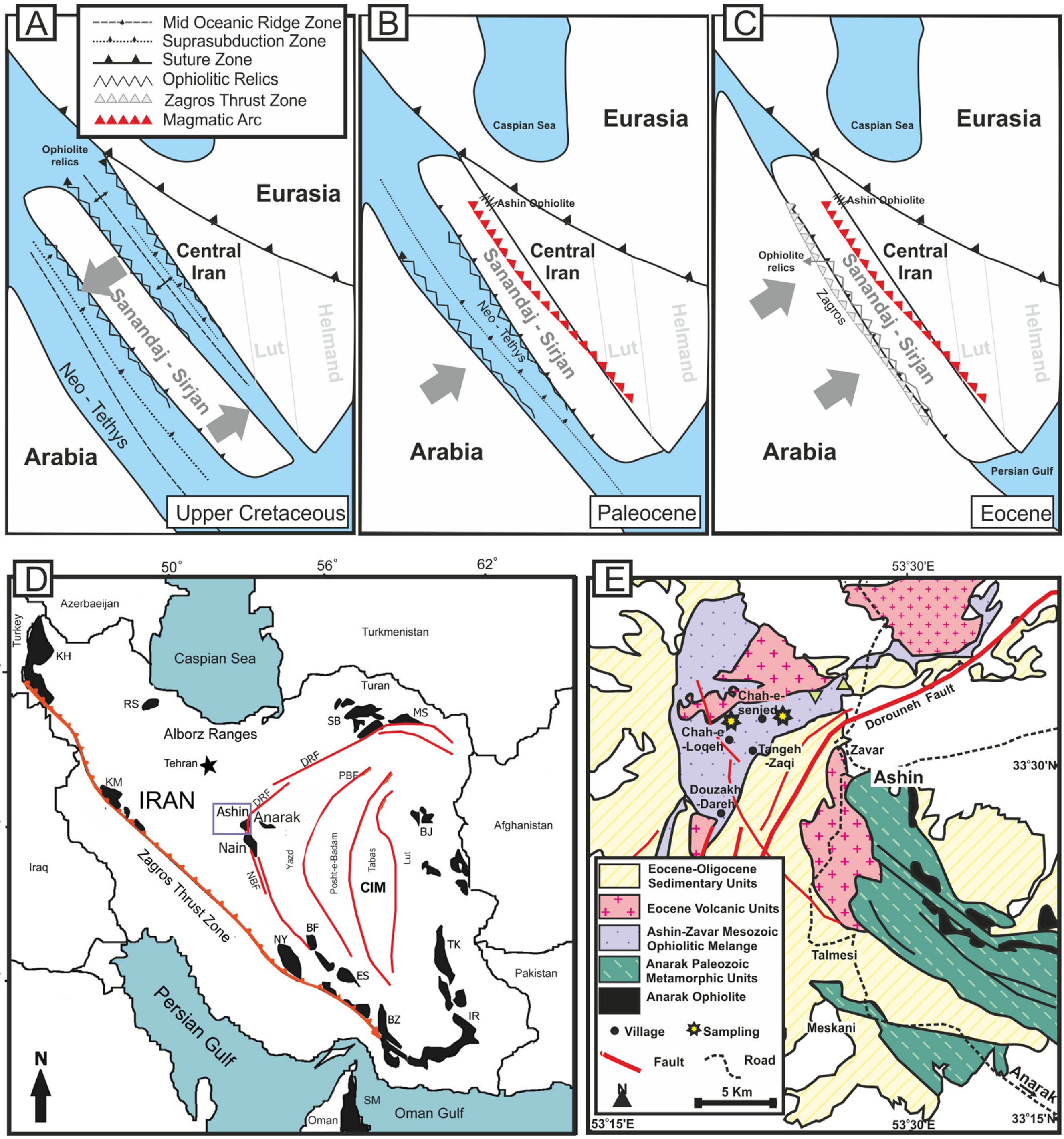

Fig. 1. (A, B, C) Schematic sketches of tectonic evolutions in eastern and western branches of Neo-Tethys Ocean in Iran, modified after Glennie (1992) and Muttoni et al. (2009); (D) Distribution of the main ophiolites in Iran including the study area of the Ashin ophiolitic mélange; (E) Geological map of colored mélange of Ashin and sample locations of the radiolarian cherts (NBF: Nain-Baft fault, DRF: Dorouneh Fault; Ophiolite abbreviations: MS = Mashhad, SB = Sabzevar, KH = Khoy, TK = Tchehel Kureh, NY = Neyriz, IR = Iranshahr, BZ = Band-e-Ziarat, ES = Esfandagheh, BF = Baft, SM = Semail, FM = Fanuj-Maskutan, JA = Jandagh).

Radiolarian microfossils, from ocean floor deposits or intercalated with pillow basalts, have been widely used in biogeochronologic investigations of the Neo-Tethyan Ocean (e.g. Tekin and Goncuoglu, 2009; Baxter et al., 2010, 2011). Radiolarian deposition (from the Middle Jurassic to latest Cretaceous) was widespread at bathyal depths (~4500–5000 m) (e.g. Turkey, Tekin and Goncuoglu (2009); Iran, Gharib and De Wever (2010); India, Baxter et al. (2010); and southern Tibet in China, Ziabrev et al. (2003, 2004). In the Ashin Ophiolite, the Cretaceous siliceous rocks occur as radiolarian cherts and radiolarites, both overlying and/or associated with Cretaceous limestones and basaltic pillow lavas. A previous report on the geology of the Anarak area (Fig. 1D) was the first limited study on the radiolarian fauna of this area (Sharkovski et al., 1984), but few details of the faunal assemblage exist. Accurate

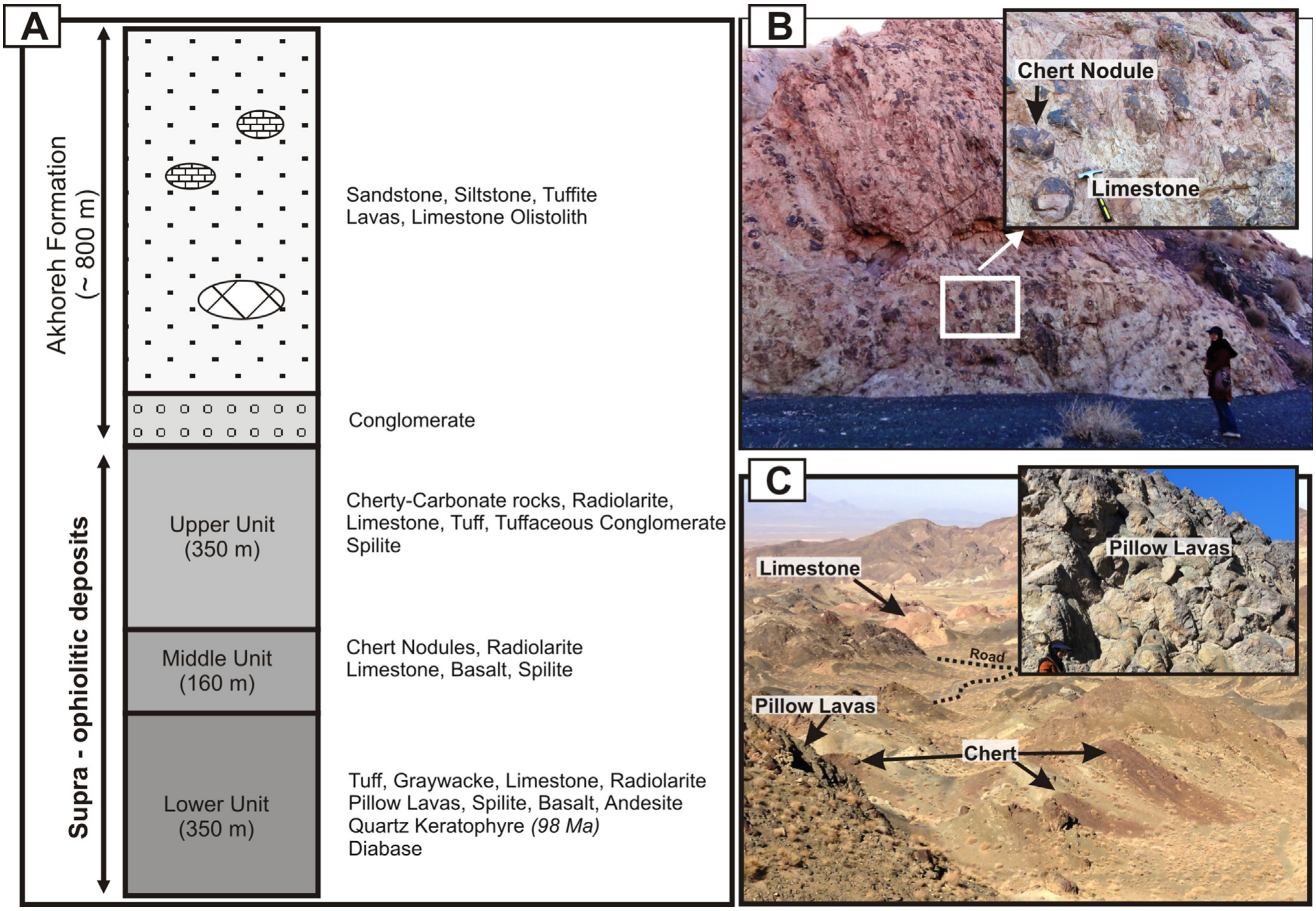

Fig. 2. (A) Cretaceous supra-ophiolitic deposits in Ashin-Zavar to Nain zone and the overlying Akhoroh Formation. Stratigraphic log is drawn based on the geological report by Sharkovski et al. (1984 and references therein); (B) Radiolarian chert nodules within the limestone in the north of Chah-e-Loqeh (view to the southwest); (C) Radiolarian chert deposits, pillow lavas, and limestones in the east Chah-e-Senjed (view to the west).

dating of deep-water deposits associated with volcanic rocks of the Ashin Ophiolite can provide valuable data to constrain the stratigraphic and paleotectonic evolution of the Neo-Tethyan oceanic basin in the west of the CEIM. Thus, the aim of this paper is to present details of the first clearly imaged mid-Cretaceous radiolarians from the Ashin Ophiolite, deposited before the closure of the eastern branch of the Neo-Tethyan oceanic basin.

2. Geological background

Mesozoic ophiolites are the most abundant ophiolites of Iran, including the Zagros ophiolites (e.g. Kermanshah (KM) and Neyriz (NY) ophiolites) and the Central Iran ophiolites (e.g. Sabzevar (SB) in the north of Central Iran, Tchehel Kureh (TK) on the eastern boundary of CEIM, and Nain and Ashin ophiolites on the western boundary of CEIM) (Fig. 1D). The ophiolitic mélange of Ashin crops out over a ~10 × 15 km^2 area located in the northwest of Anarak (Isfahan Province), to the west of Dorouneh (DRF) to Nain-Baft (NBF) faults (Fig. 1D). It is exposed amongst Eocene-Oligocene deposits, together with some Eocene volcanic rocks (Fig. 1E). This ophiolitic mélange is a dismembered and tectonised suite consisting of a relatively chaotic mixture of sedimentary, igneous, and metamorphic rocks; e.g., pelagic limestones, radiolarian cherts, basaltic lava flows and pillow lavas, diabasic dikes, plagiogranites, gabbros, pyroxenites, chromitite, mantle peridotites, marbles, schists, quartzites, skarns, banded metacherts, metagabbros, orthoamphibolites, metaperidotites, spilites, serpentinites, listwaenite, and rodingite (Shirdashtzadeh, 2014). During their complex tectonic history involving obduction and emplacement these rock units were mixed to form an ophiolite mélange.

Sharkovski et al. (1984) reported K–Ar ages for two intrusive stages in the Ashin Ophiolite ages (188 Ma (Pliensbachian, Early Jurassic) from a plagiogranite sample collected 4.6 km north-west of Zavar; and 98 Ma (Cenomanian, early Late Cretaceous) from plagiogranite and quartz-keratophyre samples collected from 4.5 km north of Zavar) (Fig. 1E). Shirdashtzadeh et al. (2011, 2014) inferred that the 188 Ma Early Jurassic age was related to an oceanic crust spreading system in which diabasic dikes and pillow lavas were erupted and covered by pelagic deposits (banded cherts, limestone, and shale succession), but a high-grade metamorphism obliterated any traces of fossils in these deposits. However, the younger 98 Ma age for plagiogranite and quartz keratophyre indicates a later phase of magmatism in the Cenomanian, when the eastern branch of the Neo-Tethyan mid oceanic spreading system reactivated melt–rock reaction and produced basalts, diabasic dikes and gabbros (Shirdashtzadeh et al., 2011, 2014). The pillow lavas of this stage crop out near Chah-e-Loqeh and Chah-e-Senjed (Fig. 1E). Geochemical data point to a MORB (mid-ocean ridge basalt) nature for the pillow lavas in this ophiolite (Shirdashtzadeh et al., 2011). In some outcrops, radiolarian cherts occur in association with pillow lavas and Upper Cretaceous limestone, but others are dispersed as deposits or layered units throughout the ophiolitic mélange.

Based on Sharkovski et al. (1984), in the most complete succession of Ashin-Zavar to Nain ophiolite zone, the Cretaceous

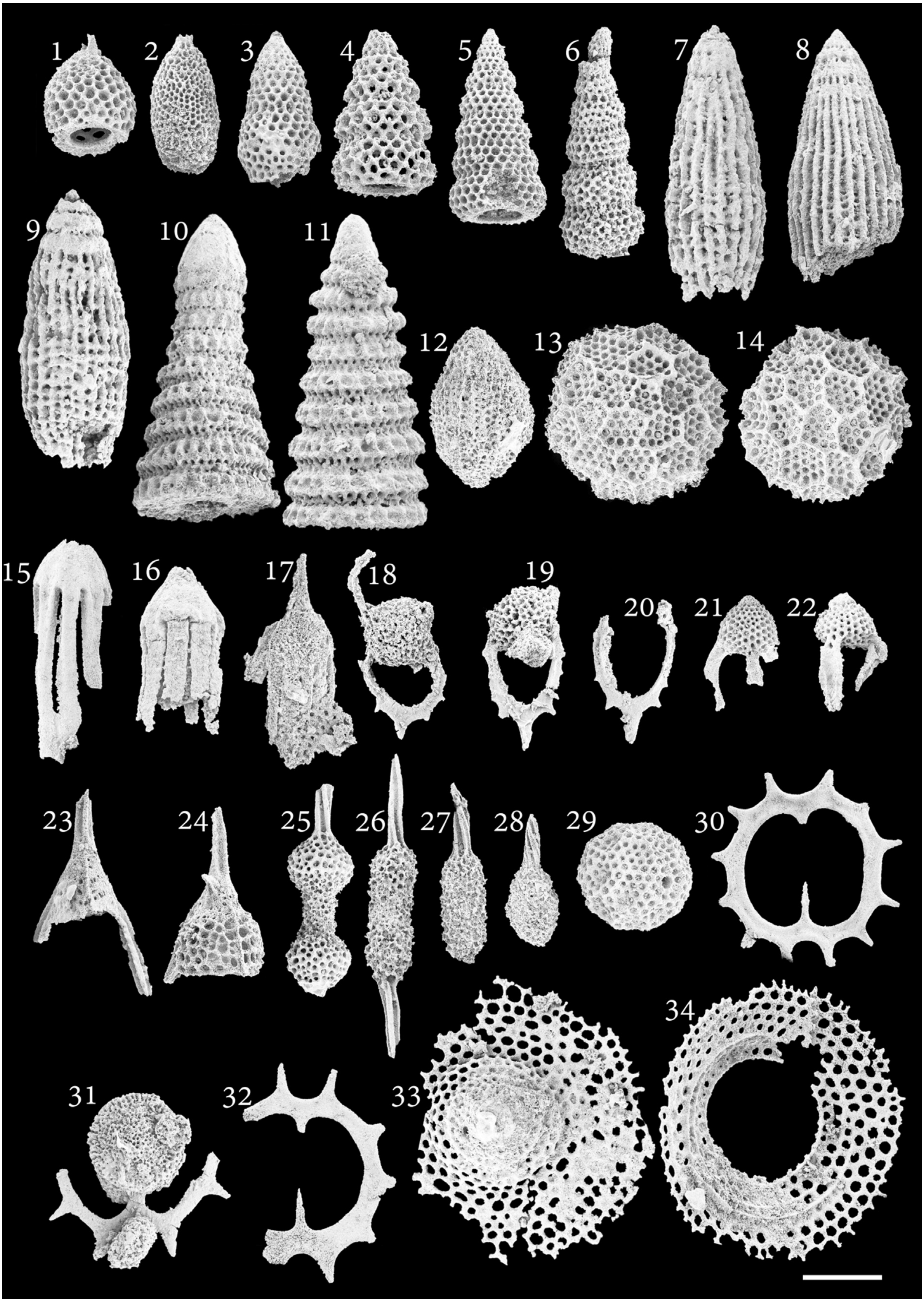

Fig. 3. Scanning electron photomicrographs of radiolarians in chert nodule sample A138 from the Ashin Ophiolite: **(A)** (1) *Rhopalosyringium hispidum* O'Dogherty (GPEM 150401); (2) *? Phalangites telum* O'Dogherty (GPEM 150402); (3–6) *Stichomitra communis* Squinabol (GPEM 150403-6); (7–9) *Dictyomitra montisserei* (Squinabol) (GPEM 150407-9); (10) *Pseudodictyomitra pseudomacrocephala* (Squinabol) (GPEM 150410); (11) *Pseudodictyomitra tiara* (Holmes) (GPEM 150411); (12) *Diacanthocapsa antiqua* (Squinabol) (GPEM 150412); (13, 14) *Archaeocenosphaera? mellifera* O'Dogherty (GPEM 150413, 150414); (15–17) *Afens liriodes* Riedel and Sanflippo (GPEM 150415-17); (18–20) *Vitorfus campbelli* Pessagno (GPEM 150418-20); (21, 22) *?Annikaella omanensis* De Wever (GPEM 150421, 150422); (23) *Ultranapora* sp. (GPEM 150423); (24) *Ultranapora cretacea* (Squinabol) (GPEM 150424); (25–27) *Archaeospongoprunum bipartitum* Pessagno (GPEM 150425-27); (28) *Archaeospongoprunum cortinaensis* Pessagno (GPEM 150428); (29) *Hemicryptocapsa polyhedra* Dumitrica (GPEM 150429); (30, 32) *Acanthocircus hueyi* (Pessagno) (GPEM 150430, 150432); (31) *Acanthocircus tympanum* O'Dogherty; (33, 34) *Sciadiocapsa speciosa* (Squinabol) (GPEM 150433, 150434). Scale bar = 100 μm.

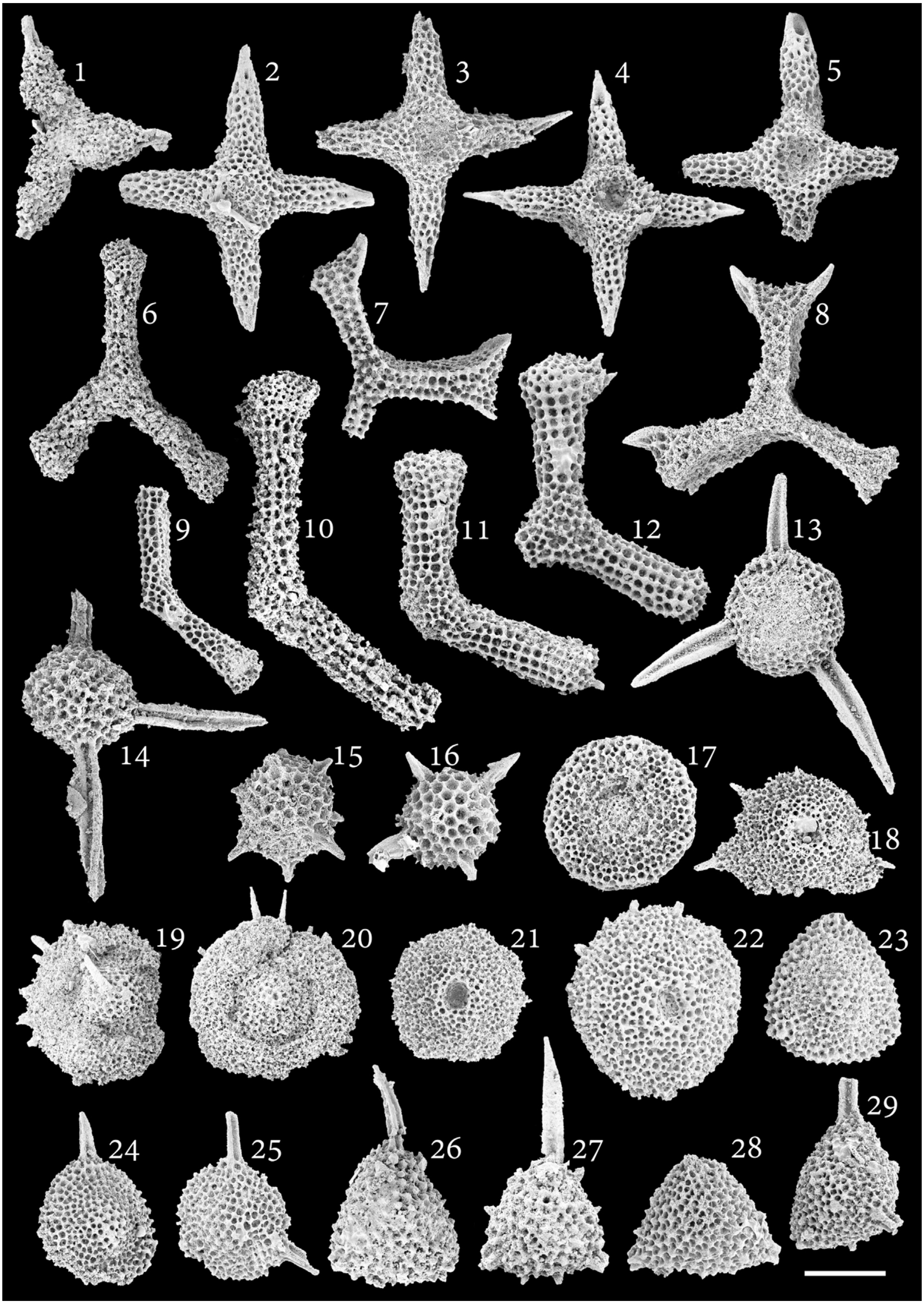

Fig. 4. Scanning electron photomicrographs of radiolarians in chert nodule sample A138 from the Ashin Ophiolite: (1) *Paronella communis* (Squinabol) (GPEM 150501); (2–5) *Crucella cachensis* Pessagno (GPEM 150502-05); (6, 9–12) *Pessagnobrachia fabianii* (Squinabol) (GPEM 150506, 150509-12); (7–8) *Halesium amissum* (Squinabol) (GPEM 150507, 150508); (13) *Triactoma hexeris* O'Dogherty (GPEM 150513); (14) *Acaeniotyle amplissima* (Foreman) (GPEM 150514); (15, 16) gen. et sp. indet. (GPEM 150516, 150516); (17) *Orbiculiforma cf. monticelloensis* Pessagno (GPEM 150517); (18–20) *Patellula ecliptica* O'Dogherty (GPEM 150518-20); (21, 22) *Patellula heroica* O'Dogherty (GPEM 150521, 150522); (23–25) *Pseudoaulophacus putahensis* Pessagno (GPEM 150523-25); (26–29) *Alievium superbum* (Squinabol) (GPEM 150526-29). Scale bar = 100 μm.

supra-ophiolitic deposits can be subdivided into upper, middle, and lower units, described in Fig. 2A. The middle unit includes basaltic rocks, chert nodules, radiolarite, and *Hedbergella* sp., *Heterohelix* sp., *Globigerina* limestones. The lower unit is composed of tuff, greywacke, limestone, radiolarite, pillow lavas, spilite, basalt, andesite, quartz keratophyre (~98 Ma; Sharkovski et al., 1984), and diabase. The upper unit includes *Globotruncana* sp. and *Globigerina* limestone, cherty-carbonate rocks, radiolarite, basalt, and andesite. The Akhoreh Formation, which overlies these Cretaceous deposits, is a chaotic unit that incorporates lower Eocene sandstone, siltstone, tuffite, lavas and limestone olistoliths (Fig. 2A).

3. Material and methods

In this study, radiolarian chert samples were selected for determination of the radiolarian fauna. Sample A138 is a brownish to dark reddish chert nodule, associated with the limestones and contains numerous well-preserved radiolarians. It was collected

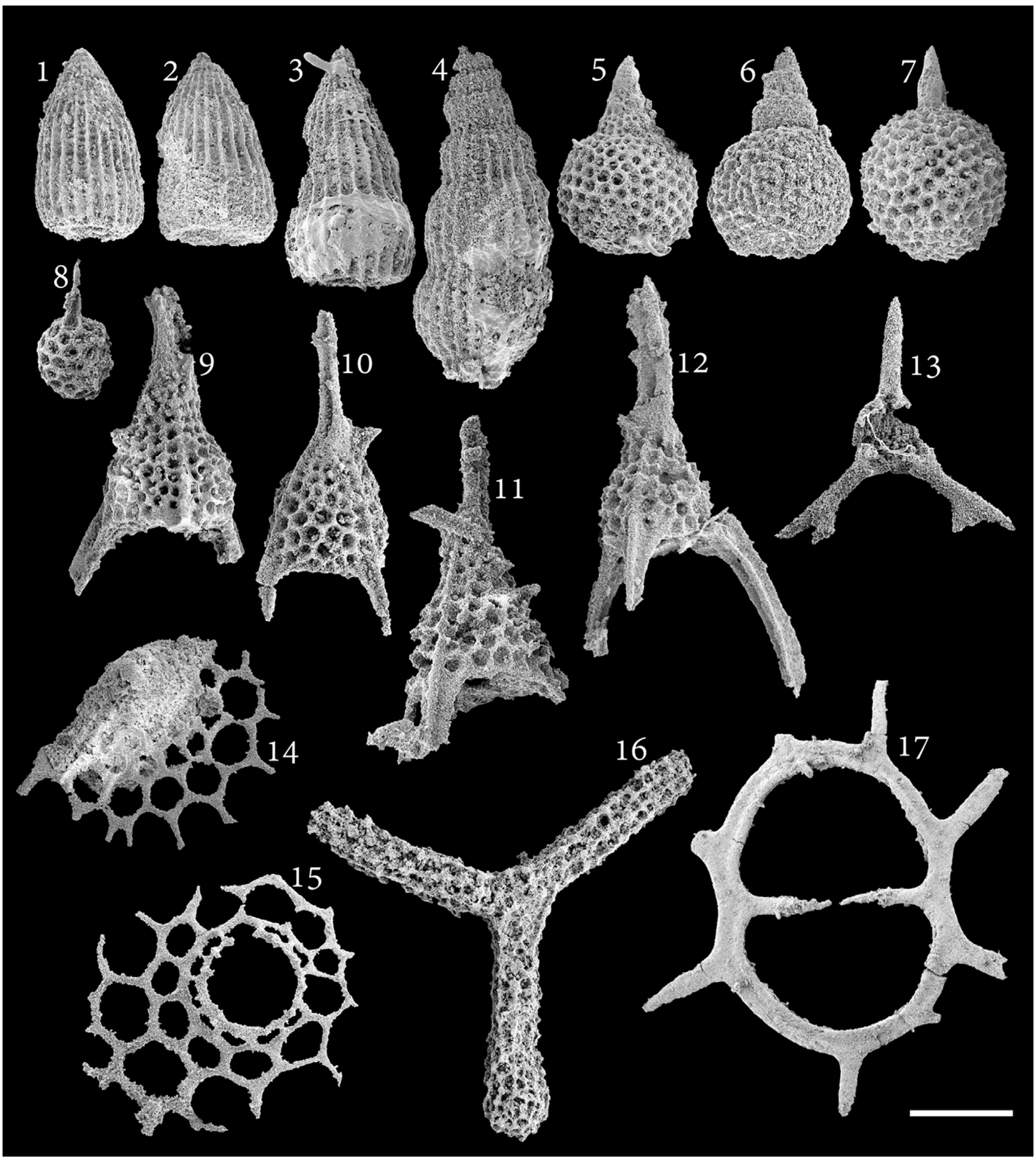

Fig. 5. Scanning electron photomicrographs of radiolarians from chert on the pillow lavas (sample A105) from the Ashin Ophiolite. (1–3) *Thanarla brouweri* (Tan) (GPEM 150601-03); (4) *Dictyomitra obesa* (Squinabol) (GPEM 150604); (5–6) *Hiscocapsa asseni* (Tan) (GPEM 150605, 150606); (7, 8) gen. et sp. Indet (GPEM 150607, 150608); (9–10) *Ultranapora cf. praespinifera* Pessagno (GPEM 150609, 150610); (11–12) *Ultranapora durhami* Pessagno (GPEM 150611, 150612); (13) *Saitoum cf. mercuriale* O'Dogherty (GPEM 150613); (14, 15) *Sciadiocapsa speciosa* (Squinabol) (GPEM 150614, 150615); (16) *Halesium cf. crassum* (Ozvoldova) (GPEM 150616); (17) *Acanthocircus levis* Donofrio and Mostler (GPEM 150617). Scale bar = 100 μm.

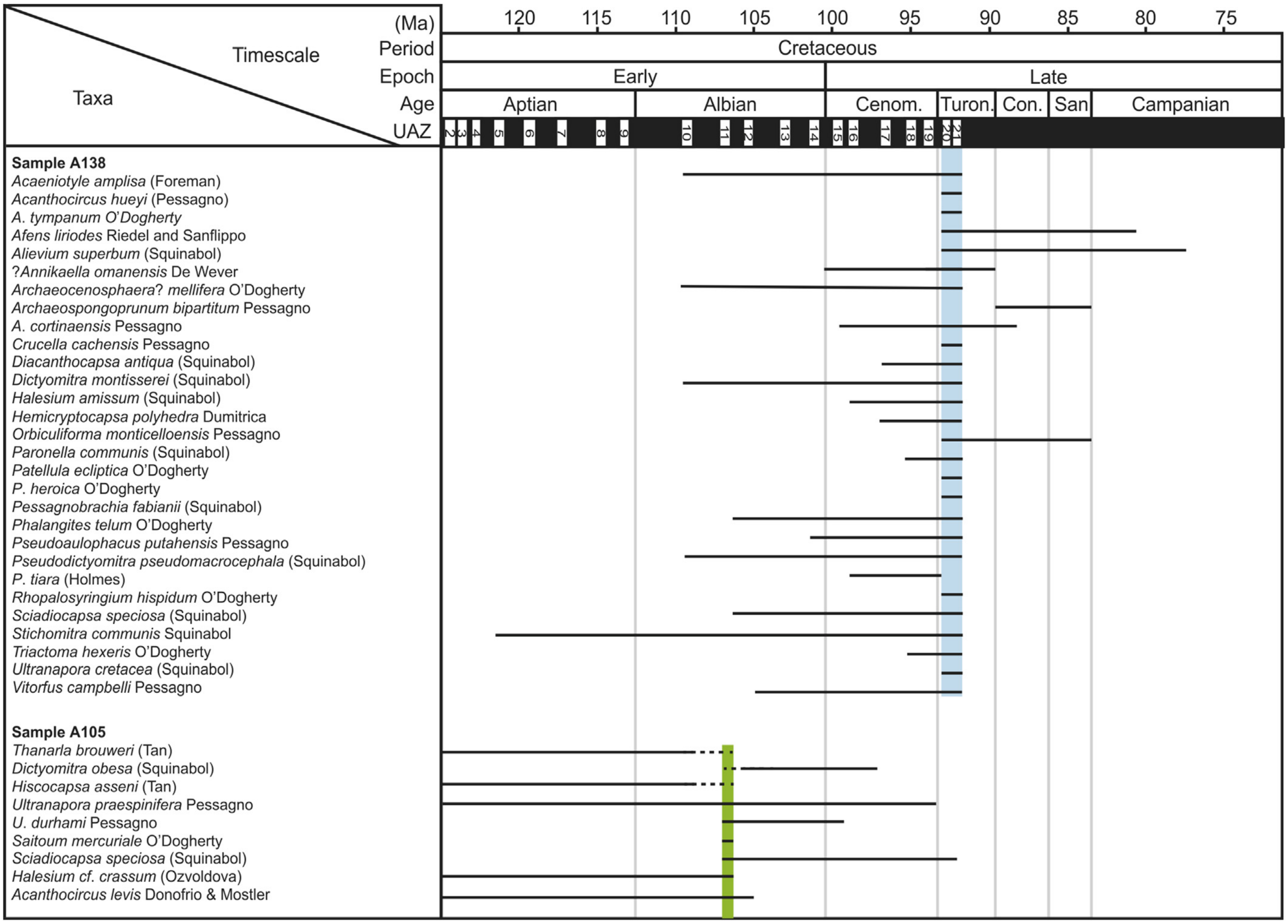

Fig. 6. Stratigraphic ranges of radiolarian taxa in the Ashin Ophiolite (Figure produced with TSCreator Pro (http://www.tscreator.org) with timescale calibrated to the 2012 Geological Time Scale of Gradstein et al. (2012)).

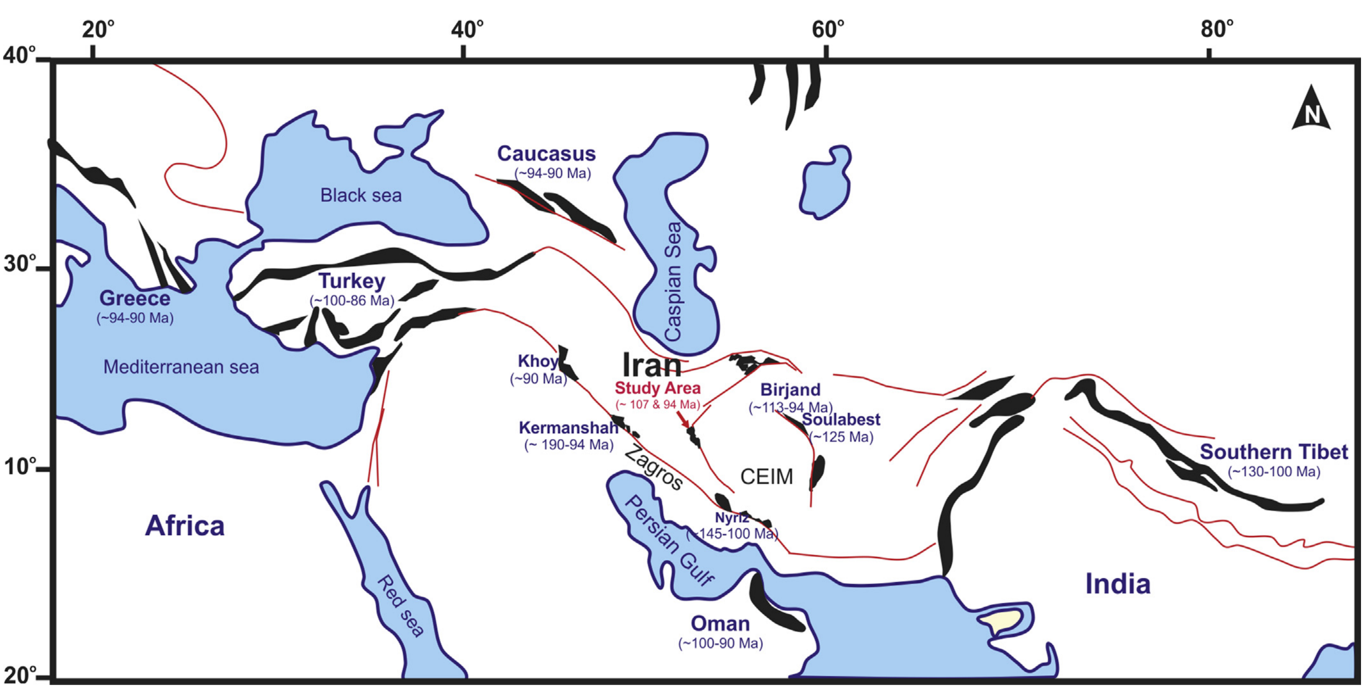

Fig. 7. Cretaceous radiolarian faunas associated with Neo-Tethyan ophiolites from Greece to Tibet.

from north of Chah-e-Loqeh (GPS 33° 31′ 21.1″ N, 053° 21′ 27.6″ E) (Fig. 2B) in a section that can be correlated with the middle unit as suggested by Sharkovski et al. (1984).

Sample A105 was selected from brownish to dark reddish chert deposits overlying pillow lavas east of Chah-e-Senjed (GPS 33° 31′ 33.2″ N, 053° 23′ 52.2″ E) (Fig. 2C) that correlate with the lower unit as suggested by Sharkovski et al. (1984).

Samples were processed in the University of Sydney Radiolarian Lab and prepared using standard radiolarian extraction techniques (Pessagno and Newport, 1972). Each sample was broken into small (1 cm^3) pieces and immersed in a <5% HF solution for 12–24 h. This was repeated, up to 10 times to capture as many radiolarian tests as possible. Tests were concentrated on a 63 μm sieve and the residue was collected. The sieves were thoroughly cleaned of all materials between each sample run. Radiolarians were picked and mounted onto an Al_2O_3 stub covered with sticky carbon tape then coated with Ti–Au alloy and photographed using a scanning electron microscope at the Australian Centre for Microscopy and Microanalysis located at the University of Sydney. The scanning electron microscope (SEM) images were compared with type specimens in the literature and an age range was compiled.

Illustrated radiolarian fossils and processed samples are curated in the collections of the School of Geography, Planning and Environmental Management (GPEM) at the University of Queensland.

4. Radiolarian fauna

Two diverse and moderately well-preserved radiolarian faunas were recovered from the samples. Radiolarians assemblages are illustrated in Figs. 3–5. Scanning electron photomicrographs of the abundant radiolarians from chert nodule samples are illustrated in Figs. 3 and 4. A less diverse, and slightly older radiolarian assemblage was also recovered from a chert layer above the pillow lavas and is illustrated in Fig. 5. The taxa identified are as follows:

Sample A105: *Thanarla brouweri* (Tan), *Dictyomitra obesa* (Squinabol), *Hiscocapsa asseni* (Tan), *Ultranapora cf. praespinifera* Pessagno, *U. durhami* Pessagno, *Saitoum cf. mercuriale* O'Dogherty, *Sciadiocapsa speciosa* (Squinabol), *Halesium cf. crassum* (Ozvoldova), *Acanthocircus levis* Donofrio and Mostler.

Sample A138: *Acaeniotyle amplisa (Foreman), Acanthocircus hueyi (Pessagno), A. tympanum O'Dogherty, Afens liriodes Riedel and Sanflippo, Alievium superbum (Squinabol), ?Annikaella omanensis De Wever, Archaeocenosphaera? mellifera O'Dogherty, Archaeospongoprunum bipartitum Pessagno, A. cortinaensis Pessagno, Crucella cachensis Pessagno, Diacanthocapsa antiqua (Squinabol), Dictyomitra montisserei (Squinabol), Halesium amissum (Squinabol), Hemicryptocapsa polyhedra Dumitrica, Orbiculiforma cf. monticelloensis Pessagno, Paronella communis (Squinabol), Patellula ecliptica O'Dogherty, P. heroica O'Dogherty, Pessagnobrachia fabianii (Squinabol), ?Phalangites telum O'Dogherty. Pseudoaulophacus putahensis Pessagno, Pseudodictyomitra pseudomacrocephala (Squinabol), P. tiara (Holmes), Rhopalosyringium hispidum O'Dogherty, Sciadiocapsa speciosa (Squinabol), Stichomitra communis Squinabol, Triactoma hexeris O'Dogherty, Ultranapora cretacea (Squinabol), Vitorfus campbelli Pessagno*.

5. Discussion

Radiolarian chert in the Ashin Ophiolite, is associated with oceanic pillow lavas and overlying limestone layers. Tucker (2001) suggested that most radiolarian chert accumulates at bathyal depots below the carbonate compensation depth (CCD) where there is no detrital or carbonate sedimentation. The nodular cherts occur in association with pelagic limestone deposits (Fig. 2B). They are possibly deep-water deposits that formed below belts of upwelling plankton-rich waters and are similar to other examples from the Mesozoic, Cenozoic and the present day (Armstrong and Brasier, 2005). In fact, better-preserved radiolarian assemblages in the nodular cherts within the overlying limestones (Fig. 2B) indicate that the basin and CCD depth of Neo-Tethys Ocean has been progressively decreased and limestones were deposited.

As the samples reported come from two different location of mélange-style outcrop it is not possible to discuss them in terms how they might contribute to our overall knowledge of radiolarian biostratigraphy. The purpose of this paper is to report their ages and the constraints these may place on the Ashin Ophiolite and formation of the mélange within which they occur. The well-established Jurassic to Cretaceous radiolarian zonations (O'Dogherty, 1994; Baumgartner et al., 1995) together with additional data on Late Cretaceous radiolarian age occurrences (Pessagno, 1976; Sanfilippo and Riedel, 1985; Schaaf, 1986; Urquhart and Banner, 1994; Hollis and Kimura, 2001; Vishnevskaya, 2001; Bragina et al., 2007; Bragina, 2009, 2012; Palechek et al., 2010; Bragina and Bragin, 2013) were used to ascertain the biostratigraphic position of radiolarians from the Ashin ophiolitic mélange cherts. Unitary Association zones (UAZ) of (O'Dogherty, 1994) correlated to the Geological Time Scale of Gradstein et al. (2012) are used. Overlapping age ranges of abundant, well-preserved taxa within the samples suggest that both were deposited during the mid-Cretaceous (Fig. 6). Sample A138 indicates an age of 94 Ma (early Turonian) while sample A105 is the oldest (107 Ma, mid-Albian). The overlapping ages of key taxa and the presence of the distinctive short-ranging taxon *Saitoum cf. mercuriale* O'Dogherty, allow correlation with UAZ11 and assignment to the mid-Albian. For Sample A138 the presence of the distinctive form *Afens liroides* Reidel and Sanfilippo together with key taxa such as *Alievium superbum* (Squinabol) allows correlation with UAZ20-21 and assignment to the Turonian *Alievium superbum* (Squinabol) radiolarian zone (O'Dogherty, 1994). Siliceous deposition occurred in a deep marine setting. Thus, this age is related to the age of the ocean after its opening but before emplacement of the ophiolite onto a continental margin. This age suggests that the lower rock units (i.e. pillow lavas and basalts) may be even older than 94 Ma and 107 Ma, as Sharkovski et al. (1984) obtained 98 Ma age (Cenomanian) for some of the final phases of plagiogranite and quartz keratophyre associated with this ophiolite.

The faunal assemblages from the eastern branch of Neo-Tethys in the west of the CEIM (Ashin Ophiolite) show similarity to some other radiolarian faunas associated with Neo-Tethyan ophiolites elsewhere, e.g. Greece (Turonian; Bandini et al., 2006), Caucasus (Turonian; Zhamoida et al., 1976), Crimea and Turkey (Cenomanian – Coniacian; Bragina, 2004), Oman (Cenomanian-Turonian; De Wever et al., 1988), southern Tibet (Barremian – Albian; Ziabrev et al., 2003, 2004), as well as the radiolarian assemblages in the western branch of Neo-Tethys Oceanic Basin in Iran (i.e. "Outer Zagros Ophiolitic Belt", including early Coniacian in Khoy complex, Pessagno et al., 2005; early Pliensbachian – Turonian in Kermanshah formation, Gharib and De Wever, 2010; Berriasian – Cenomanian in Neyriz ophiolite, Babaei et al., 2005), and the ophiolites in the east of CEIM along the Sistan suture zone (e.g., early Aptian in Soulabest ophiolite, Babazadeh and De Wever, 2004a,b; Albian – Cenomanian in Birjand ophiolite, Babazadeh, 2007) (Fig. 7).

6. Conclusions

Chert layers and nodules overlying pillow lavas of Ashin Ophiolite (in the eastern branch of the Tethyan Ocean in Iran) accumulated in the mid-Cretaceous in a deep marine setting. Radiolarian microfossil ages are consistent with radiometric ages previously obtained for associated plagiogranites and quartz keratophyre. The mid-Cretaceous (Albian UAZ11 and Turonian UAZ20-21) radiolarian assemblages from the Ashin Ophiolite are comparable to other radiolarian faunas from Cretaceous Neo-Tethyan ophiolites in Greece, Turkey, Iran (Outer Zagros Ophiolitic Belt in Iran, e.g. Khoy, Kermanshah, Neyriz, and Soulabest), and southern Tibet.

Acknowledgments

We thank Prof. Ghodrat Torabi (University of Isfahan) for his support in fieldwork and Mr. Tom Savage for his assistance in the WHS compliant processing of radiolarian samples at the University of Sydney. The authors also acknowledge the facilities and the scientific and technical assistance of the Australian Centre for Microscopy and Microanalysis Research at the University of Sydney. The authors express gratitude to the constructive reviews of Dr. Sergey Zyabrev, and one anonymous reviewer, and the editorial handling of Editor, Dr. Eduardo Koutsoukos, which improved the original manuscript.

References

Agard, P., Omrani, J., Jolivet, L., Whitechurch, H., Vrielynck, B., Spakman, W., Monie, P., Meyer, B., Wortel, R., 2011. Zagros orogeny: a subduction-dominated process. Geological Magazine 148 (5–6), 692–725.
Armstrong, H., Brasier, M., 2005. Microfossils. Blackwell Publishing Ltd, p. 296.
Babaei, A., Babaei, H.A., Arvin, M., 2005. Tectonic evolution of the Neyriz ophiolite, Iran: An accretionary prism model. Ofioliti 30 (2), 65–74.
Babazadeh, S.A., 2007. Cretaceous radiolarians from Birjand ophiolitic range in Sahlabad province, eastern Iran. Revue de Paléobiologie 26, 89–98.
Babazadeh, S.A., De Wever, P., 2004a. Radiolarian Cretaceous age of Soulabest radiolarites in ophiolite suite of eastern Iran. Bulletin de la Société Géologique de France. Série VIII 175, 121–129.
Babazadeh, S.A., De Wever, P., 2004b. Early Cretaceous radiolarian assemblages from radiolarites in the Sistan Suture (eastern Iran). Geodiversitas 26, 185–206.
Bandini, A.N., Baumgartner, P.O., Caron, M., 2006. Turonian radiolarians from Karnezeika, Argolis Peninsula, Peloponnesus (Greece). Eclogae Geologicae Helvetiae 99 (1), 1–20.
Baumgartner, P.O., O'Dogherty, L., Gorican, S., Urquhart, E., Pillevuit, A., De Wever, P., 1995. Middle Jurassic to Lower Cretaceous Radiolaria of Tethys: Occurrence, Systematics, Biochronology. Mémoires de Géologie, 23. Universite de Lausanne, pp. 1–1172.
Baxter, A.T., Aitchison, J.C., Ali, J.R., Zyabrev, S.V., 2010. Early Cretaceous radiolarians from the Spongtang massif, Ladakh, NW India: implications for Neo-Tethyan evolution. Journal of the Geological Society, London 167, 511–517.
Baxter, A.T., Aitchison, J.C., Zyabrev, S.V., Ali, J.R., 2011. Upper Jurassic radiolarians from the Naga Ophiolite, Nagaland, northeast India. Gondwana Research 20 (2–3), 638–644.
Bragina, L.G., 2004. Cenomanian-Turonian radiolarians of northern Turkey and the Crimean Mountains. Paleontological Journal 38, 325–456.
Bragina, L.G., 2009. Radiolarians and stratigraphy of Cenomanian-Coniacian deposits in the Crimean and West Sakhalin Mountains, Pt. 2: Comparative analysis. Stratigraphy and Geological Correlation 17, 430–442.
Bragina, L.G., 2012. Radiolarian biostratigraphy of the Perapedhi Formation (Cyprus): implications for the geological evolution of the Troodos Ophiolite. Bulletin de la Societe Geologique de France 183, 343–348.
Bragina, L.G., Bragin, N.Y., 2013. New data on the Albian-Cenomanian radiolarians from the Karai Formation (South India). Stratigraphy and Geological Correlation 21, 515–530.
Bragina, L.G., Agarkov, Y.V., Bragin, N.Y., 2007. Radiolarians of the Upper Cenomanian and Lower Turonian from Deposits of the Ananuri Formation, the Western Caucasus (Lazarevskoe Area). Stratigraphy and Geological Correlation 15, 310–320.
Chen, X., Wang, C., Hu, X., Huang, Y., Wang, P., Luba, J., Zeng, X., 2007. Cretaceous oceanic red beds, distribution, lithostratigraphy and paleoenvironments. Acta Geologica Sinica 81 (6), 1070–1086.
De Wever, P., Bourdillon-De Grissac, C., Beurrier, M., 1988. Radiolaires sénoniens de la nappe de Samail (Oman). Revue de Micropaléontologie 31, 166–179.
Gharib, F., De Wever, P., 2010. Mesozoic radiolarians from the Kermanshah Formation (Iran). Comptes Rendus Palevol 9, 209–219.
Ghasemi, A., Talbot, C.J., 2006. A new tectonic scenario for the Sanandaj-Sirgan zone, Iran. Journal of Asian Earth Sciences 26, 683–693.
Glennie, K.W., 1992. Plate Tectonics and the Oman Mountains. Tribulus 2 (2), 11–21.
Gradstein, F.M., Ogg, J.G., Schmitz, M., Ogg, G., 2012. The Geologic Time Scale 2012. Elsevier, p. 1176.
Hollis, C.J., Kimura, K., 2001. A unified radiolarian zonation for the Late Cretaceous and Paleocene of Japan. Micropaleontology 47 (3), 235–255.
Jansa, L., Hu, X.M., 2009. Cretaceous pelagic black shales and red beds of the North Atlantic: origins, paleoclimate and paleoceanographic implications. In: Hu, X.M., Wang, C., Scott, R.W., Wagreich, M., Jansa, L. (Eds.), Cretaceous oceanic red beds: stratigraphy, composition, origins, and paleoceanographic and paleoclimatic significance. SEPM Special, 91, pp. 59–72.
Muttoni, G., Mattei, M., Balini, M., Zanchi, A., Gaetani, M., Berra, F., 2009. The drift history of Iran from the Ordovician to the Triassic. In: Brunet, M.F., Wilmsen, M., Granath, J.W. (Eds.), South Caspian to Central Iran Basins. Geological Society, 312. Special Publications, London, pp. 7–29.
O'Dogherty, L., 1994. Biochronology and Paleontology of Mid-Cretaceous Radiolarians from Northern Apennines (Italy) and Betic Cordillera (Spain). Mémoires de Géologie Universite de Lausanne 21, 1–415.
Palechek, T., Savel'ev, D., Savel'eva, O., 2010. Albian-Cenomanian Radiolarian Assemblage from the Smaginsk Formation, the Kamchatskii Mys Peninsula of Eastern Kamchatka. Stratigraphy and Geological Correlation 18, 63–82.
Pessagno, E.A., Newport, R.L., 1972. A technique for extracting Radiolaria from radiolarian cherts. Micropaleontology 18, 231–234.
Pessagno, E.A., 1976. Radiolarian zonation and stratigraphy of the Upper Cretaceous portion of the Great Valley Sequence, California Coast Ranges, 2. Micropaleontology, Special Publication, pp. 1–95.
Pessagno, E.A.J., Ghazi, A.M., Kariminia, M., Duncan, R.A., Hassanipak, A.A., 2005. Tectonostratigraphy of the Khoy Complex, northwestern Iran. Stratigraphy 2, 49–63.
Reichert, J., 2007. A metallogenetic model for carbonate-hosted non-sulphide zinc deposits based on observations of Mehdi Abad and Irankuh, Central and Southwestern Iran. Dissertation. Martin-Luther-Universität Halle-Wittenberg, p. 157.
Sanfilippo, A., Riedel, W.R., 1985. Cretaceous Radiolaria. In: Bolli, H.M., Saunders, J.B., Perch-Nielsen, K. (Eds.), Plankton Stratigraphy. Cambridge University Press, Cambridge/New York/New Rochelle/Melbourne/Sydney, pp. 573–630.
Schaaf, A., 1986. Radiolaria from Deep Sea Drilling Project Leg 89. In: Moberly, R., Schlanger, S.O., et al. (Eds.), Initial Reports of the Deep Sea Drilling Project, Volume 89. U.S. Government Printing Office, Washington, D.C, pp. 321–326.
Sharkovski, M., Susov, M., Krivyakin, B., 1984. Geology of the Anarak area (Central Iran), Explanatory text of the Anarak quadrangle map, 1:250,000, V/O Technoexport Report 19. Geological Survey of Iran, Tehran, p. 143.
Shirdashtzadeh, N., 2014. Petrology of pillow lavas and amphibolites and metamorphism in mantle peridotites of Nain and Ashin ophiolites. Ph.D. Thesis in Petrology. Department of Science, University of Isfahan, Iran, p. 345.
Shirdashtzadeh, N., Torabi, G., Arai, S., 2010. Metamorphism and metasomatism in the Jurassic of Nain ophiolitic mélange, Central Iran. Neues Jahrbuch für Geologie und Paläontologie-Abhandlungen 255 (3), 255–275.
Shirdashtzadeh, N., Torabi, G., Arai, S., 2011. Two Mesozoic oceanic phases recorded in the basic and metabasic rocks of the Nain and Ashin-Zavar ophiolitic mélanges (Isfahan Province, Central Iran). Ofioliti 36 (2), 191–205.
Shirdashtzadeh, N., Torabi, G., Meisel, T.C., Arai, S., Bokhari, S.N.H., Samadi, R., Gazel, E., 2014. Origin and evolution of metamorphosed mantle peridotites of Darreh Deh (Nain Ophiolite, Central Iran): Implications for the Eastern Neo-Tethys evolution. Neues Jahrbuch für Geologie und Paläontologie-Abhandlungen 273 (1), 89–120.
Stocklin, J., 1974. Northern Iran: Alborz Mountain, Mesozoic-Cenozoic orogenic Belts, data for orogenic studies. Geological Society Special Publication (London) 4, 213–234.
Stoneley, R., 1975. On the origin of ophiolite complexes in the Southern Tethys region. Tectonophysics 25, 303–322.
Tekin, U.K., Goncuoglu, M.C., 2009. Late Middle Jurassic (Late Bathonian-early Callovian) radiolarian cherts from the Neotethyan Bornova flysch zone, Spil Mountains, Western Turkey. Stratigraphy and Geological Correlation 17 (3), 298–308.
Torabi, G., 2004. Petrology of Anarak area ophiolites (NE of Isfahan Province, Iran). Ph, D, Thesis in Petrology. Tarbiat Modares University, Tehran, Iran, p. 240.
Tucker, M.E., 2001. Sedimentary petrology: an introduction to the origin of sedimentary rocks, 3rd edition. Blackwell, Oxford, p. 262.
Urquhart, E., Banner, F.T., 1994. Biostratigraphy of the supra-ophiolite sediments of the Troodos Massif, Cyprus: the Cretaceous Peraphedhi, Kannaviou, Moni and Kathikas Formations. Geological Magazine 131, 499–518.
Vishnevskaya, V.S., 2001. Jurassic to Cretaceous radiolarian biostratigraphy of Russia, Russian Academy of Sciences. Institute of the Lithosphere of Marginal Seas, GEOS, Moscow, p. 376.
Zhamoida, A.I., Kazintsova, L.I., Tikhomirova, L.B., 1976. Kompleksy Mezozoiskikh radiolyarii Malogo Kavkaza [Complexes of Mesozoic radiolarians of the Lesser Caucasus]. Izvestiya Akademii Nauk SSSR, Moscow. Seriya Geologicheskaya 2, 156–160.
Ziabrev, S.V., Aitchison, J.C., Abrajevitch, A., Badengzhu, Davis, A.M., Luo, H., 2003. Precise radiolarian age constraints on the timing of ophiolite generation and sedimentation in the Dazhuqu terrane, Yarlung-Tsangpo suture zone, Tibet. Journal of the Geological Society, London 160, 591–599.
Ziabrev, S.V., Aitchison, J.C., Abrajevitch, A., Badengzhu, Davis, A.M., Luo, H., 2004. Bainang Terrane, Yarlung-Tsangpo suture, southern Tibet (Xizang, China): a record of intra-Tethyan subduction-accretion processes preserved on the roof of the World. Journal of the Geological Society, London 161, 523–539.